Investigation of a Multi-Modular IPT System on the Efficiency and Current Balancing due to Inter–/Cross Coupling

Calvin Riekerk
Electrical Sustainable Energy dept.
Delft University of Technology
Delft, The Netherlands
C.Riekerk@tudelft.nl

Jianning Dong
Electrical Sustainable Energy dept.
Delft University of Technology
Delft, The Netherlands
J.Dong-4@tudelft.nl

Thiago Batista Soeiro
Faculty of EEMCS
University of Twente
Enschede, The Netherlands
T.Batistasoeiro@utwente.nl

Pavol Bauer
Electrical Sustainable Energy dept.
Delft University of Technology
Delft, The Netherlands
P.Bauer@tudelft.nl

2023 IEEE Energy Conversion Congress and Exposition (ECCE) | 979-8-3503-1644-5/23/$31.00 ©2023 IEEE | DOI: 10.1109/ECCE53617.2023.10362509

***Abstract*—Inductive power transfer systems can process higher power using multiple charging pad modules connected in parallel. However, the effects on the system operation of the inter-/cross coupling among the pads have to be studied. This paper analyses the power transfer efficiency and current distribution of a quadruple modular IPT system. Additionally, a sensitivity analysis of the power transfer efficiency is provided based on the tolerances of the secondary resonant capacitors. The analysis shows that the efficiency of a multi-modular IPT system will increase compared to a single module and that there would not be a negligible imbalance in the current due to the inter-/cross coupling. In the experiments, the results of the quadruple modular IPT system's estimated AC efficiency are lower than a single module. It also shows that the could be bifurcation when multiple modules are deployed. Both can be attributed to the mismatch in resonant frequency, self-inductance and main mutual inductance between the modules. Future work will focus on mitigating the circulating currents caused by the mismatch between modules.**

***Index Terms*—Inductive Power Transfer, Inter–/Cross Coupling, Modular Design.**

I. Introduction

Inductive power transfer (IPT) has risen in popularity in recent years [1]. There has been considerable success in pushing the research in IPT systems to 20 kW [2]–[5]. However, some work still needs to be done to ensure that IPT systems can be used for ultra-fast battery charging at much higher power. For example, in a user case of the opportunity charging of buses, the short interval while the passengers hop on/off the bus is used for ultra-fast charging at high power (200 kW) to reduce the battery size. The IPT technology could provide several advantages in this application compared to contact charging, such as less vulnerability to weather effects and vandalism [6].

High power brings challenges to the power electronics and charging pads design. The high charging power increases the current throughout the whole system. This makes it challenging to achieve high efficiency because of limited conductor areas. A potential solution could be to use multiple parallel modules to increase the power level [7]–[11]. However, the inter-/cross coupling between the charging pads can affect the current sharing between each module, hence the efficiency will also be influenced [12]. This paper evaluates the current sharing between the modules and its effect on the efficiency.

This paper will investigate the efficiency as mentioned above and the current sharing problem. An analysis concerning the multi-module IPT system is provided in Section II. The simulation results for the efficiency and current sharing are explained in Section III. The experimental results are discussed in Section IV Lastly, the conclusion is given in Section V.

This project has received funding from the Electronic Components and Systems for European Leadership Joint Undertaking under grant agreement No. 876868. This Joint Undertaking receives support from the European Union's Horizon 2020 research and innovation programme and Germany, Slovakia, Netherlands, Spain, Italy.

II. Analysis

The multi-module IPT system is shown in Fig. 1. Synchronous rectification is used in the system in order to improve the efficiency of the secondary side power electronics. Furthermore, series-series compensation is utilized for its simple design while contributing to low input resistance, no circulating current, and independence on the load and coupling coefficient [13]–[15].

In this example, four modules of 50 kW will be used. (1) can be used assuming that each of the four modules outputs a power of 50 kW, the same DC voltage supply and that all the converters are synchronized [16], [17]. In addition, it is assumed that the same resonant frequency is assumed.

$$\begin{bmatrix} V_{AB} \\ 0 \\ \vdots \\ V_{AB} \\ 0 \end{bmatrix} = \begin{bmatrix} A(1,2) & B \\ B^T & A(3,4) \end{bmatrix} \begin{bmatrix} I_{AB,1} \\ I_{ab,1} \\ \vdots \\ I_{AB,4} \\ I_{ab,4} \end{bmatrix}, \quad (1)$$

$$A = \begin{bmatrix} Z_{1x} & -j\omega M_x & j\omega M_{1x1y} & -j\omega M_{1x2y} \\ -j\omega M_x & Z_{2x} & -j\omega M_{2x1y} & j\omega M_{2x2y} \\ j\omega M_{1x1y} & -j\omega M_{2x1y} & Z_{1y} & -j\omega M_y \\ -j\omega M_{1x2y} & j\omega M_{2x2y} & j\omega M_y & Z_{2y} \end{bmatrix}. \quad (2)$$

$$B = \begin{bmatrix} j\omega M_{1113} & -j\omega M_{1123} & j\omega M_{1114} & -j\omega M_{1124} \\ -j\omega M_{2113} & j\omega M_{2123} & -j\omega M_{2114} & j\omega M_{2124} \\ j\omega M_{1213} & -j\omega M_{1223} & j\omega M_{1214} & -j\omega M_{1224} \\ -j\omega M_{2213} & j\omega M_{2223} & -j\omega M_{2214} & j\omega M_{2224} \end{bmatrix}, \quad (3)$$

where:

$$Z_{1n} = R_{1n} + j\left(\frac{(\omega^2 - \omega_0^2)L_p}{\omega}\right), \quad (4)$$

$$Z_{2n} = R_{2n} + R_{Lac} + j\left(\frac{(\omega^2 - \omega_0^2)L_s}{\omega}\right), \quad (5)$$

$$R_{Lac} = \frac{8}{\pi^2}\frac{V_{out}^2}{P_{out}}. \quad (6)$$

where M_{abcd} is the mutual inductance between coil ab and cd, ω is the angular operating frequency and ω_0 is the angular resonant frequency. The following equations can be used to analyze the power transfer efficiency when it is assumed that the current distribution at all the Tx and Rx modules is even provided that the ratio between the main coupling and inter-/cross coupling is sufficiently high. This will later be verified in the simulation. The real part of the reflected impedance on one of the Tx side modules is given by:

Where the complex part of the Rx side is:

$$X_s = \omega(L_{2n} + M_{2n2x} + M_{2n2y} + M_{2n2z}) - \frac{1}{\omega C_{2n}}. \quad (8)$$

The power transfer efficiency between the Tx and Rx side circuits is calculated by:

$$\eta_{pt} = \frac{Re(Z_r)}{Re(Z_r) + R_{1n}}\frac{R_{Lac}}{R_{Lac} + R_2}. \quad (9)$$

As indicated from (7)–(9), the reflected impedance will increase because of the additional mutual inductances due to the inter-/cross coupling. So, in the end, the high-frequency AC power transfer efficiency of a multi-modular IPT system should be higher than a traditional IPT system which implies an advantage when using multiple modules.

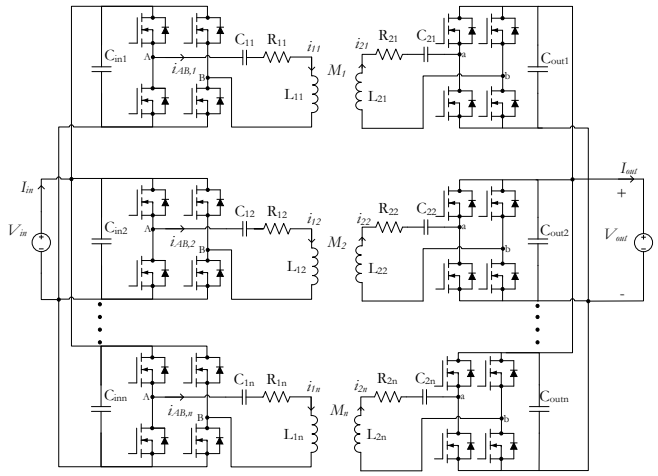

Fig. 1: Multi-module IPT system.

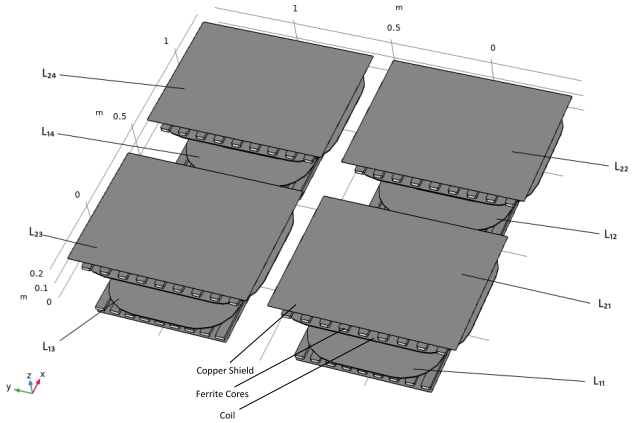

Fig. 2: The multi-module IPT system in Comsol 5.4.

A. Sensitivity analysis

In practice, the values of the resonant components will suffer from some tolerance, resulting in uneven current distribution and potentially lowering the overall efficiency and power transfer. Fig. 3 illustrates the power transfer efficiency for different secondary compensation tolerances, with a range of +/- 5 %, against the normalized frequency. Furthermore, the nominal, minimum and maximum capacitances are also marked. The results show that the multi-modular IPT system will typically outperform the efficiency of a singular even with a tolerance. Another key point is that the efficiency could increase for lower secondary capacitance around the nominal frequency. A lower capacitance could potentially reduce X_s due to the inter-/cross coupling which corresponds with (7)–(9).

III. Simulation

In order to determine the efficiency and AC current through each module, (1) will be used. The inductances in Fig. I have been obtained using the multi-physics software Comsol 5.4. A minimal distance of 10 cm has been used between the charging pads in order to account for the mechanical constraints due

$$Re(Z_r) = \frac{\omega^2(M_n + M_{2n1x} + M_{2n1y} + M_{2n1z})(M_n + M_{1n2x} + M_{1n2y} + M_{1n2z})(R_{Lac} + R_{2n})}{(R_{Lac} + R_{2n})^2 + X_s^2}. \quad (7)$$

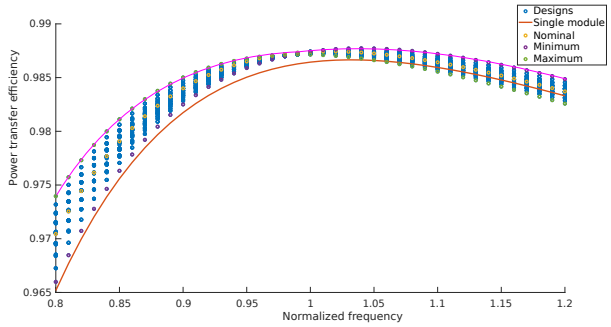

Fig. 3: Scatter plot for different secondary capacitor tolerances dependent on the normalized frequency and power transfer efficiency.

TABLE I: The inductances of the multi-module IPT system.

	L/M [μH]
$L_{11} = L_{12} = L_{13} = L_{14}$	169.11
$L_{21} = L_{22} = L_{23} = L_{24}$	154.23
$M_1 = M_2 = M_3 = M_4$	54.423
$M_{1113} = M_{1214}$	0.62598
$M_{2122} = M_{2324}$	2.8960
$M_{1123} = M_{1224}$	0.48531
$M_{2113} = M_{2214}$	0.48062
$M_{1114} = M_{1213}$	0.15485
$M_{2123} = M_{2224}$	1.3338
$M_{1112} = M_{1314}$	4.7901
$M_{1124} = M_{1223}$	0.32460
$M_{2114} = M_{2213}$	0.32333
$M_{1122} = M_{2314}$	3.2818
$M_{2112} = M_{1324}$	3.2772
$M_{2124} = M_{2223}$	0.43974

to the casing. The configuration of the four charging pads pairs is shown in Fig. 2 and the obtained self and mutual inductances are displayed in Table I which assumes that the self-inductances and main mutual inductances are the same between each module.

The results of the study have been compared with a simulation in GeckoCircuits in order to verify the theoretical implications. The high-frequency AC power efficiency comparison between a single module and four 50 kW modules is 98.64 % and 98.74 % respectively. It can be observed that the high-frequency AC power transfer efficiency would slightly improve due to the cross-coupling between the Tx and Rx sides. This is in compliance with the analysis in (7)–(9). Moreover, the current sharing between each module is almost even which validates the assumptions in (7)–(9). The AC voltages and currents have been simulated in the simulator GeckoCircuits to verify this.

TABLE II: The measured inductances of the down-scaled multi-module IPT system.

	L/M [μH]		M [μH]		M [μH]
L_{11}	59.8907	M_{1112}	1.3928	M_{1213}	0.3178
L_{21}	59.848	M_{1122}	1.1768	M_{1223}	0.2763
L_{12}	59.9738	M_{1113}	0.8353	M_{1214}	1.0298
L_{22}	60.5607	M_{1123}	0.5480	M_{1224}	0.5795
L_{13}	60.3181	M_{1114}	0.3143	M_{1322}	0.2833
L_{23}	58.0948	M_{1124}	0.328	M_{2223}	0.2883
L_{14}	58.1566	M_{2112}	1.0118	M_{1422}	0.5730
L_{24}	59.1183	M_{2122}	1.3323	M_{2224}	1.0573
M_1	17.5365	M_{2113}	0.5115	M_{1314}	1.6283
M_2	18.2194	M_{2123}	0.8605	M_{1324}	1.2805
M_3	17.5365	M_{2114}	0.2605	M_{1423}	1.116
M_4	18.3743	M_{2124}	0.3065	M_{1424}	1.4118

IV. Experimental Results

A. Experimental Setup

A downscaled version of the setup consisting of H-bridge-converters, compensation capacitors and charging pads has been constructed to validate the theoretical analysis in Sections II and III. However, there are some key differences between the experimental setup and the analysis which are the following:

1) The self and mutual inductances of the downscaled setup are smaller, but the coupling factors are as close as possible to the simulated values in order to keep the comparison as fair as possible.
2) Instead of each module having its own converter, a single H-bridge converter is utilized at both the Tx and Rx sides, as displayed in Fig. 4. This configuration enhances the DC-DC efficiency when deploying a single module due to reduced power at the same voltage. Consequently, the overall converter loss is significantly lower compared to the scenario where multiple modules are deployed. The H-bridge converters make use of IMZ120R030M1H SiC MOSFETs, where three of these MOSFETs are connected in parallel.

The measured inductances are shown in Table II and the setup is displayed in Fig. 4.

B. Results & Discussion

The measured waveforms of the AC voltage at the converter outputs and the AC current of a single module are shown in Fig. 5(a) and Fig. 5(b) also shows the AC voltage at the converter outputs and the total AC current of four modules connected in parallel. One of the key differences is that the IPT system with a singular module is able to ensure zero voltage switching (ZVS) turn-on while the waveform in Fig. 5(b) shows that there is hard switching at turn-on despite the inductive behavior. This might, in turn imply that the system is in bifurcation when multiple modules are connected in parallel. Further inspection is necessary in order to confirm that it is the case.

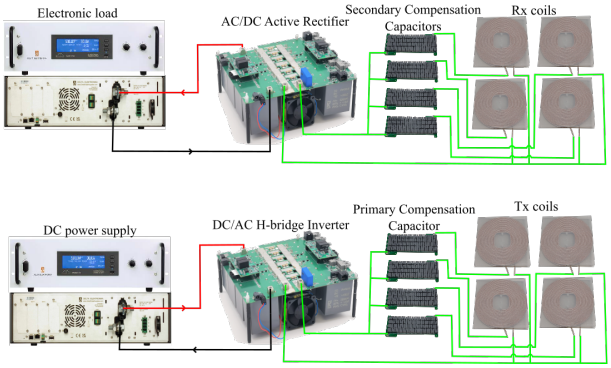

Fig. 4: Experimental setup of the downsized multi-modular IPT system.

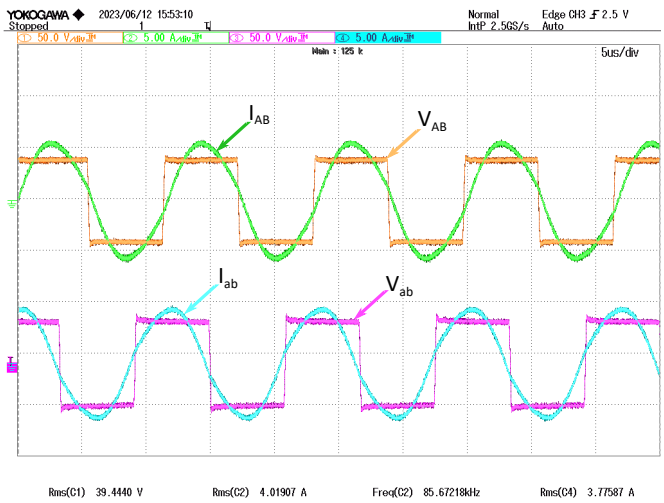

(a)

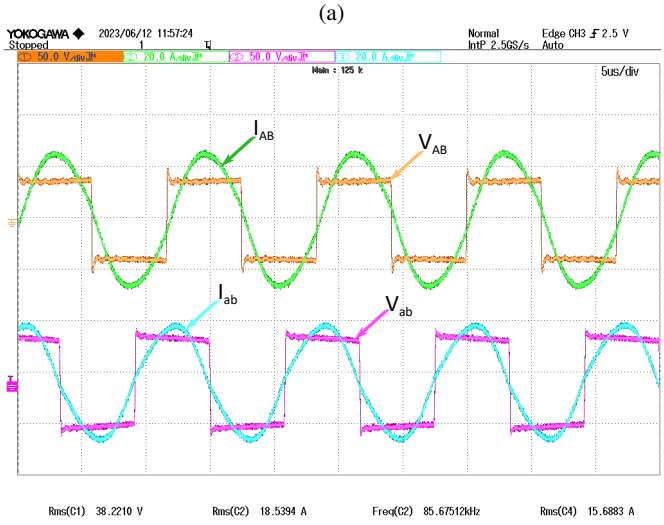

(b)

Fig. 5: (a) Measured waveforms of a single module and (b) four modules.

It is difficult to measure the efficiency of the high-frequency AC stage of the IPT system due to the limited bandwidth of the oscilloscope and probes. In order to reach ensure ZVS it is mandatory that the inverter and rectifier show inductive and capacitive behavior. Hence, the high-frequency AC voltage and current are never in phase with each other, which can result in a small phase error between them. Even a small phase error will result in a large error when the power is calculated during post-processing, making the result unreliable.

A different approach to estimating the efficiency of the high-frequency AC stage is by calculating the losses in the H-bridge converters and either adding or substracting them from the DC output and input power. The total conduction losses of an H-bridge converter are calculated using the following:

$$P_{cond} = 2I_{AB}^2 R_{DS,ON,eq}(I_{AB}, T_j), \tag{10}$$

where T_j is the junction temperature and $R_{DS,ON,eq}$ is the equivalent drain-source resistance of the MOSFET. The total switching losses are estimated by:

$$P_{sw} = Nf(E_{ON}(V_{DS}, I_{ON}, T_j) + E_{OFF}(V_{DS}, I_{OFF}, T_j)), \tag{11}$$

where V_{DS} is the drain-source voltage over the MOSFET, I_{ON} is the current at the MOSFET at turn-on, I_{OFF} is the turn-off current of the MOSFET, N is the number of MOSFETs in the H-bridge converter, f is the operating frequency of the H-bridge converter, E_{ON} is the turn-on energy of the MOSFET and E_{OFF} is the turn-off energy which both can be found in the datasheet of the MOSFET.

TABLE III: Comparison between the power and efficiency measurements and estimation of a single module and four modules.

	DC-DC measurement		AC-AC estimation	
	Single module	Four modules	Single module	Four modules
Pin [W]	140.68	637.7	140.36	620.64
Pout [W]	134.72	573.6	135.01	588.73
η [%]	95.760	89.955	96.19	94.86

The DC-DC power and efficiency measurements are given in Table III together with the estimated AC power and efficiency using the DC-DC measurements in Table III, (10) and (11). It can be seen that there is still a significant difference in the efficiency between a singular and four modules which can be attributed to circulating current due to the parallel connection of the modules. These circulating currents could be caused by the difference in self-inductance and resonant frequency between each module which deviates from the assumptions made in Section II and III. Nevertheless, a more precise measurement should be done in the future since the switching losses are hard to determine. A calorimetric box will be built as it will provide a much more accurate loss measurement.

V. Conclusion & Future Work

In this paper, an analysis of a quadruple modular IPT system has been given. This included the efficiency of the system and the current in each module. The analysis shows that the efficiency of the multi-modular IPT system will increase

compared to a single module due to the inter-/cross coupling. Furthermore, the imbalance in the current would be insignificant. In experiments, it is shown that it is difficult to measure the high-frequency AC efficiency. Instead, an estimation is made using the DC-DC power measurements. The experiments show that the AC efficiency reduces when multiple modules are deployed in comparison to the single module case. This could be caused by the deviation in resonant frequency, self-inductance and main mutual inductance between the modules, which was not taken into account in the analysis. For future work, a calorimetric box will be built in order to obtain accurate measurement results for the high-frequency AC efficiency. Additionally, more research will be done on the mitigation of circulating current when multiple modules are deployed. Lastly, the bifurcation that appears when multiple modules are used will be studied on how to mitigate this.

REFERENCES

[1] H. Feng, R. Tavakoli, O. C. Onar, and Z. Pantic, "Advances in high-power wireless charging systems: Overview and design considerations," *IEEE Transactions on Transportation Electrification*, vol. 6, no. 3, pp. 886–919, 2020.

[2] S. Y. Choi, S. Y. Jeong, B. W. Gu, G. C. Lim, and C. T. Rim, "Ultraslim s-type power supply rails for roadway-powered electric vehicles," *IEEE Transactions on Power Electronics*, vol. 30, no. 11, pp. 6456–6468, 2015.

[3] M. Mohammad, O. C. Onar, G.-J. Su, J. Pries, V. P. Galigekere, S. Anwar, E. Asa, J. Wilkins, R. Wiles, C. P. White, and L. E. Seiber, "Bidirectional lcc–lcc-compensated 20-kw wireless power transfer system for medium-duty vehicle charging," *IEEE Transactions on Transportation Electrification*, vol. 7, no. 3, pp. 1205–1218, 2021.

[4] B. Goeldi, J. Tritschler, and S. Reichert, "Measurement results of a 22 kw bidirectional inductive charger," in *Proceedings of PCIM Europe 2015; International Exhibition and Conference for Power Electronics, Intelligent Motion, Renewable Energy and Energy Management*, 2015, pp. 1–8.

[5] W. Shi, J. Dong, T. B. Soeiro, C. Riekerk, F. Grazian, G. Yu, and P. Bauer, "Design of a highly efficient 20-kw inductive power transfer system with improved misalignment performance," *IEEE Transactions on Transportation Electrification*, vol. 8, no. 2, pp. 2384–2399, 2022.

[6] H. H. Wu, A. Gilchrist, K. D. Sealy, and D. Bronson, "A high efficiency 5 kw inductive charger for evs using dual side control," *IEEE Transactions on Industrial Informatics*, vol. 8, no. 3, pp. 585–595, 2012.

[7] A. Calabro, B. Cohen, A. Daga, J. Miller, and F. McMahon, "Performance of 200-kw inductive charging system for range extension of electric transit buses," in *2019 IEEE Transportation Electrification Conference and Expo (ITEC)*, 2019, pp. 1–5.

[8] J. Shin, S. Shin, Y. Kim, S. Ahn, S. Lee, G. Jung, S.-J. Jeon, and D.-H. Cho, "Design and implementation of shaped magnetic-resonance-based wireless power transfer system for roadway-powered moving electric vehicles," *IEEE Transactions on Industrial Electronics*, vol. 61, no. 3, pp. 1179–1192, 2014.

[9] J. H. Kim, B.-S. Lee, J.-H. Lee, S.-H. Lee, C.-B. Park, S.-M. Jung, S.-G. Lee, K.-P. Yi, and J. Baek, "Development of 1-mw inductive power transfer system for a high-speed train," *IEEE Transactions on Industrial Electronics*, vol. 62, no. 10, pp. 6242–6250, 2015.

[10] H. Hao, G. A. Covic, and J. T. Boys, "A parallel topology for inductive power transfer power supplies," *IEEE Transactions on Power Electronics*, vol. 29, no. 3, pp. 1140–1151, 2014.

[11] T. Shijo, K. Ogawa, M. Suzuki, Y. Kanekiyo, M. Ishida, and S. Obayashi, "Emi reduction technology in 85 khz band 44 kw wireless power transfer system for rapid contactless charging of electric bus," in *2016 IEEE Energy Conversion Congress and Exposition (ECCE)*, 2016, pp. 1–6.

[12] G. Ning, K. Zhao, and M. Fu, "A passive current sharing method for multitransmitter inductive power transfer systems," *IEEE Transactions on Industrial Electronics*, vol. 69, no. 5, pp. 4617–4626, 2022.

[13] V. Shevchenko, O. Husev, R. Strzelecki, B. Pakhaliuk, N. Poliakov, and N. Strzelecka, "Compensation topologies in ipt systems: Standards, requirements, classification, analysis, comparison and application," *IEEE Access*, vol. 7, pp. 120 559–120 580, 2019.

[14] W. Li, H. Zhao, J. Deng, S. Li, and C. C. Mi, "Comparison study on ss and double-sided lcc compensation topologies for ev/phev wireless chargers," *IEEE Transactions on Vehicular Technology*, vol. 65, no. 6, pp. 4429–4439, 2016.

[15] C.-S. Wang, O. Stielau, and G. Covic, "Design considerations for a contactless electric vehicle battery charger," *IEEE Transactions on Industrial Electronics*, vol. 52, no. 5, pp. 1308–1314, 2005.

[16] Y. Li, R. Mai, L. Lu, T. Lin, Y. Liu, and Z. He, "Analysis and transmitter currents decomposition based control for multiple overlapped transmitters based wpt systems considering cross couplings," *IEEE Transactions on Power Electronics*, vol. 33, no. 2, pp. 1829–1842, 2018.

[17] A. Hossain, P. Darvish, S. Mekhilef, K. S. Tey, and C. W. Tong, "A new coil structure of dual transmitters and dual receivers with integrated decoupling coils for increasing power transfer and misalignment tolerance of wireless ev charging system," *IEEE Transactions on Industrial Electronics*, vol. 69, no. 8, pp. 7869–7878, 2022.